Supplementary Information

Control of Electronic Properties of 2D Carbides (MXenes) by Manipulating Their Transition Metal Layers

Babak Anasori[1,2], Chenyang Shi[3], Eun Ju Moon[1], Yu Xie[4], Cooper A. Voigt[1], Paul R. C. Kent[4,5], Steven J. May[1], Simon J. L. Billinge[3,6], Michel W. Barsoum[1], Yury Gogotsi[1,2]*

[1]Department of Materials Science & Engineering, Drexel University, Philadelphia, PA 19104, United States
[2]A.J. Drexel Nanomaterials Institute, Drexel University, Philadelphia, PA 19104, United States
[3]Department of Applied Physics and Applied Mathematics, Columbia University, New York, NY 10027, United States
[4]Center for Nanophase Materials Sciences, Oak Ridge National Laboratory, Oak Ridge, TN 37381, United States
[5]Computer Science and Mathematics Division, Oak Ridge National Laboratory, Oak Ridge, TN 37381, United States
[6]Condensed Matter Physics and Materials Science Department, Brookhaven National Laboratory, Upton, NY 11973, United States

*Corresponding author:
Y. Gogotsi (gogotsi@drexel.edu) Tel.: +1-215-895-6446 Fax: +1-215-895-1934

I. X-ray diffraction results

X-ray diffraction (XRD) was carried out on the as filtered delaminated d-$Mo_2TiC_2T_x$ and d-$Mo_2Ti_2C_3T_x$ films using a Rigaku Smartlab (Tokyo, Japan) diffractometer with Cu-Kα radiation (40 KV and 44 mA); step scan 0.02º, 3°–65° 2 theta range, step time of 1 s, 10x10 mm^2 window slit.

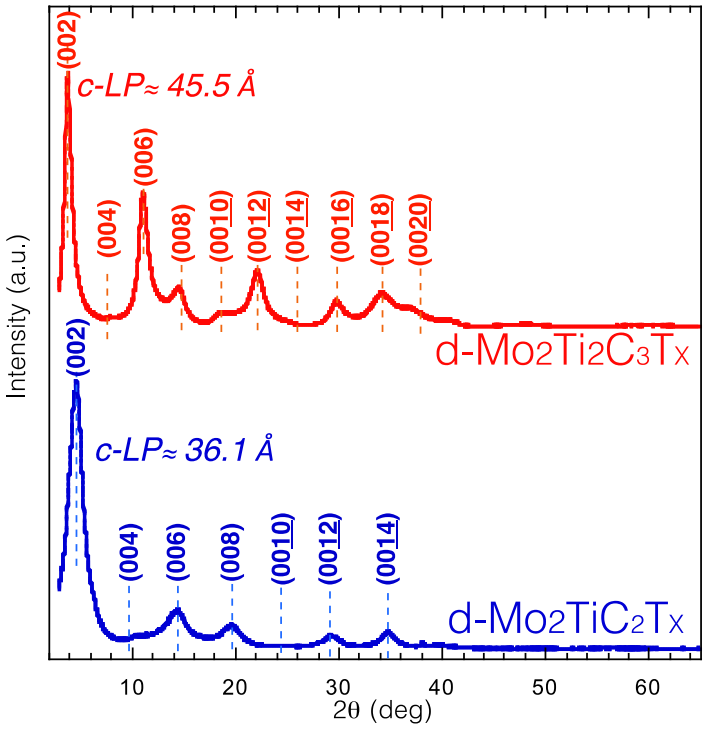

Figure S1. XRD patterns of the delaminated d-$Mo_2TiC_2T_x$ (bottom, blue) and d-$Mo_2Ti_2C_3T_x$ (top, red).

II. Undistorted structures of $Mo_2TiC_2T_x$ and $Mo_2Ti_2C_3T_x$

Figure S2 represents the undistorted $Mo_2TiC_2T_x$ and $Mo_2Ti_2C_3T_x$ structures based on numbers presented in Table 2. *c* lattice parameters were calculated using the XRD results (Figure S1). Large spacing between MXene layers shows a large number of intercalant layers, possibly up to 3 layers of water.

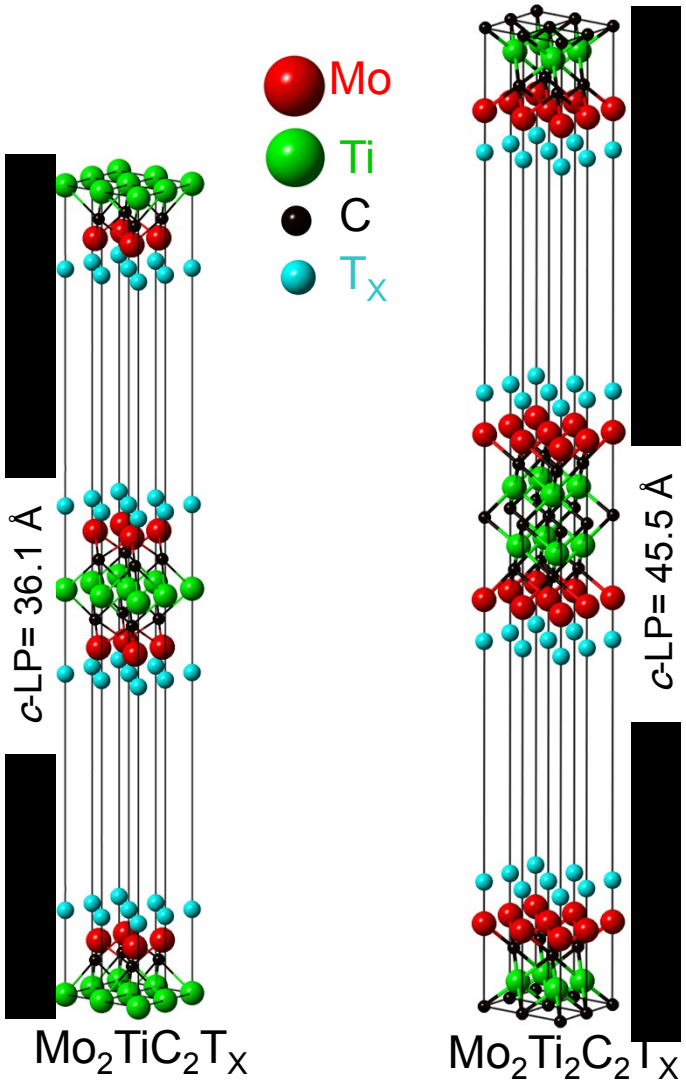

Figure S2. Structures of $Mo_2TiC_2T_x$ and $Mo_2Ti_2C_3T_x$. T_x represents the surface terminations (O, F and OH) depicted in blue.

II. Resistivity vs temperature fitting for $Mo_2TiC_2T_x$

Figure S3 shows the fitting results of the temperature dependent resistivity to the equation, $\rho = \rho_0 exp[(T_0/T)^m]$, where ρ_0 is a prefactor. The exponent, m, is indicative of the conduction model with simple activation, Efros-Shklovskii (E-S) variable range hopping (VRH), 2D VRH, and 3D VRH yielding m = 1, 0.5, 0.33, and 0.25, respectively.[1,2] Additionally, the resistivity is fit to a power-law model [Fig. S3(d)], $\rho = AT^p$, where A and p are constants. The power-law dependence is the only model that reproduces the data, albeit over a limited 20 – 100 K temperature range. The physical origin of the power-law behavior is unclear at this time.

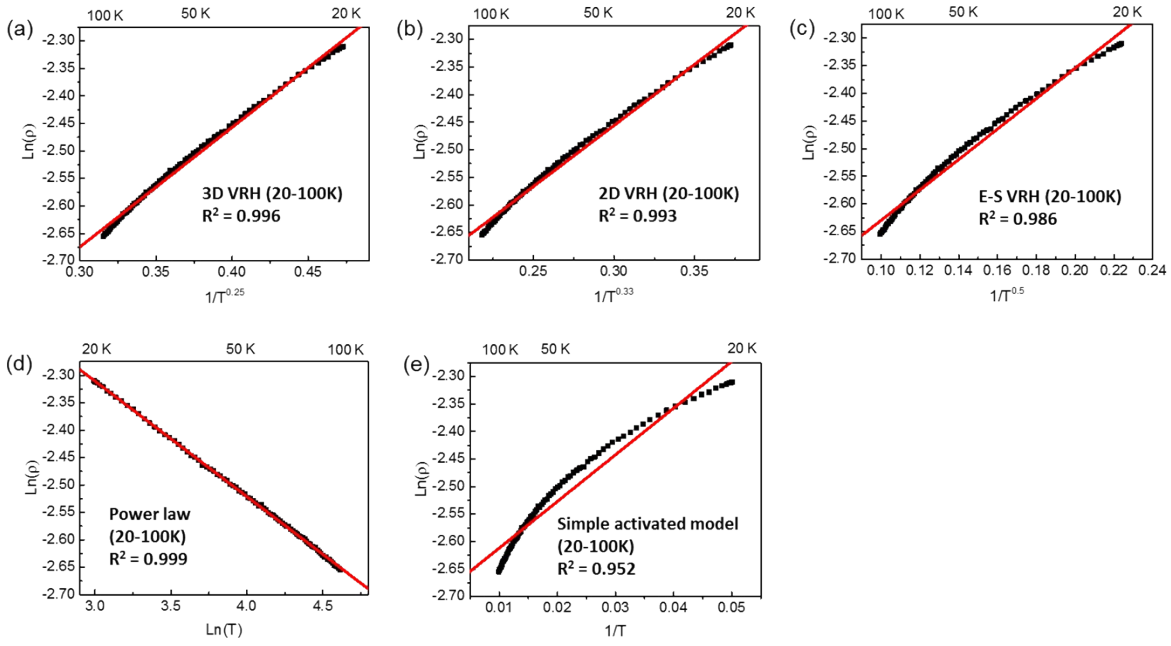

Figure S3. Resistivity fitting of a ML-$Mo_2TiC_2T_x$ over the temperature range from 20 to 100 K in (a) 3D VRH, (b) 2D VRH, (c) E-S VRH, (d) power law, and (e) simple activated models.

III. Detailed DFT calculated results

Figure S4 represents the crystal structure of monolayer $Mo_2TiC_2O_2$, which was used for magnetic simulations.

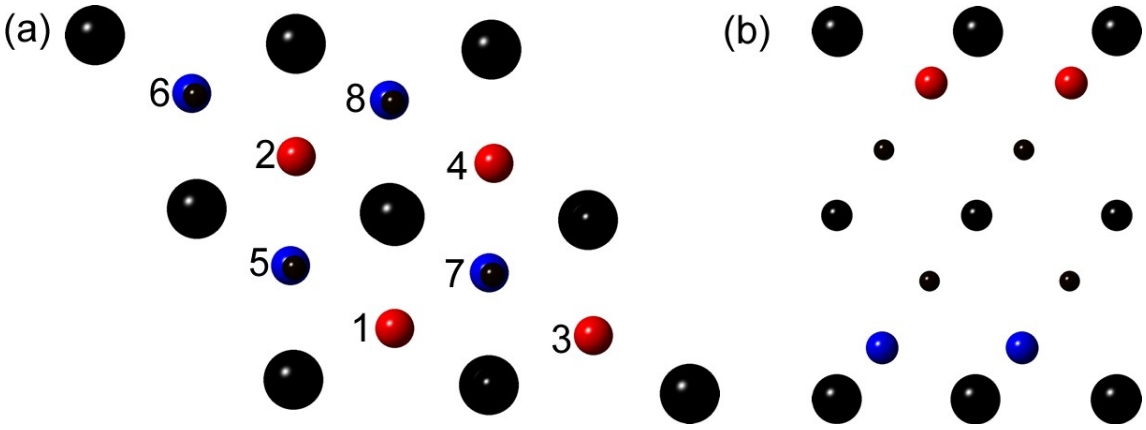

Figure S4. Top (a) and side (b) views of $Mo_2TiC_2O_x$. Mo atoms in the upper layer are in red, and that in lower layer are in blue. Other atoms are shown in black.

Table S1 shows the considered magnetic orderings in our simulations.

Table S1. Considered magnetic orderings. +, spin up; -, spin down.

Type	1	2	3	4	5	6	7	8
NM	0	0	0	0	0	0	0	0
FM	+	+	+	+	+	+	+	+
AFM1	+	+	+	+	-	-	-	-
AFM2	+	+	-	-	+	+	-	-
AFM3	+	+	-	-	-	-	+	+
AFM4	+	-	-	+	+	-	-	+
AFM5	+	-	-	+	-	+	+	-
AFM6	+	-	+	-	+	-	+	-
AFM7	+	-	+	-	-	+	-	+

The corresponding total energies of these magnetic states are shown in Table S2.

Table S2. Calculated total energies (eV/f.u.) of Mo-MXenes with different magnetic ordering. The lowest total energy of each MXene is listed in bold (reference to NM state).

	NM	**FM**	**AFM1**	**AFM2**	**AFM3**	**AFM4**	**AFM5**	**AFM6**	**AFM7**
$Mo_2TiC_2(OH)_2$	0.000	-0.384	-0.461	-0.673	-0.567	-0.444	**-0.677**	-0.673	-0.567
$Mo_2TiC_2O_2$	0.000	-0.186	-0.196	-0.387	-0.386	-0.395	**-0.385**	-0.385	-0.306
$Mo_2TiC_2F_2$	0.000	-0.342	-0.535	-0.521	-0.401	-0.402	**-0.583**	-0.521	-0.402
$Mo_2TiC_2(OH)_{1.5}F_{0.5}$	0.000	-0.044	-0.092	**-0.184**	-0.178	-0.168	-0.146	-0.167	-0.173
$Mo_2TiC_2(OH)F$	0.000	-0.095	-0.347	-0.410	-0.304	-0.334	-0.410	**-0.419**	-0.304
$Mo_2TiC_2O_{1.5}F_{0.5}$	0.000	-0.368	-0.245	-0.560	-0.560	-0.560	-0.552	-0.560	**-0.568**
Mo_2TiC_2OF	0.000	-0.161	-0.389	-0.366	-0.235	-0.389	**-0.416**	-0.366	-0.412
$Mo_2Ti_2C_3(OH)_2$	0.000	0.070	0.117	-0.239	-0.237	-0.235	-0.258	-0.248	**-0.312**
$Mo_2Ti_2C_3O_2$	0.000	-0.201	-0.223	-0.451	-0.450	**-0.462**	-0.449	-0.451	-0.450
$Mo_2Ti_2C_3F_2$	0.000	-0.962	-1.036	-1.189	**-1.223**	-1.185	-1.213	-1.185	-1.219
$Mo_2Ti_2C_3(OH)_{1.5}F_{0.5}$	0.000	-0.051	-0.182	-0.151	-0.179	-0.181	-0.173	**-0.193**	-0.179
$Mo_2Ti_2C_3(OH)F$	0.000	-0.242	-0.105	**-0.267**	-0.250	-0.216	-0.213	-0.252	-0.254
$Mo_2Ti_2C_3O_{1.5}F_{0.5}$	0.000	-0.117	-0.082	-0.121	-0.119	-0.083	-0.120	-0.119	**-0.129**
$Mo_2Ti_2C_3OF$	0.000	-0.130	0.321	**-0.148**	-0.137	0.008	0.011	0.006	0.006

The lattice parameters of the non-magnetic and most stable magnetic states are listed and compared with experimental data. The predicted values are slightly bigger due to the GGA and Hubbard U approximations. The overall agreement is good.

Table S3. Calculated lattice parameters (Å) compared with experiments.

MXene		*a*	*r*(Mo-C)	*r*(C-Ti)	*r*(Mo-O/F)
$Mo_2TiC_2T_x$	Exp.	2.935	2.022	2.259	2.142
$Mo_2TiC_2(OH)_2$	NM	3.078	2.171	2.218	2.247
	AFM5	3.172	2.209	2.252	2.268
$Mo_2TiC_2O_2$	NM	3.040	2.120	2.189	2.150
	AFM4	3.135	2.205	2.193	2.147
$Mo_2TiC_2F_2$	NM	3.039	2.161	2.210	2.254
	AFM5	3.198	2.178	2.223	2.272
$Mo_2TiC_2(OH)_{1.5}F_{0.5}$	NM	3.063	2.138	2.219	2.226
	AFM2	3.099	2.196	2.221	2.250
$Mo_2TiC_2(OH)F$	NM	3.061	2.116	2.192	2.224
	AFM6	3.150	2.182	2.219	2.237
$Mo_2TiC_2O_{1.5}F_{0.5}$	NM	3.067	2.156	2.220	2.156
	AFM7	3.166	2.218	2.228	2.119
Mo_2TiC_2OF	NM	3.039	2.183	2.181	2.230
	AFM5	3.076	2.221	2.199	2.218
$Mo_2Ti_2C_3T_x$		2.959	2.130	2.111	1.916
$Mo_2Ti_2C_3(OH)_2$	NM	3.091	2.158	2.121	2.212
	AFM7	3.151	2.184	2.177	2.274
$Mo_2Ti_2C_3O_2$	NM	3.071	2.175	2.182	2.129
	AFM4	3.125	2.202	2.197	2.150
$Mo_2Ti_2C_3F_2$	NM	3.058	2.127	2.189	2.281
	AFM3	3.149	2.186	2.220	2.249
$Mo_2Ti_2C_3(OH)_{1.5}F_{0.5}$	NM	3.081	2.140	2.183	2.242
	AFM6	3.105	2.144	2.195	2.259
$Mo_2Ti_2C_3(OH)F$	NM	3.083	2.103	2.157	2.189
	AFM2	3.104	2.130	2.157	2.222
$Mo_2Ti_2C_3O_{1.5}F_{0.5}$	NM	3.085	2.083	2.139	2.158
	AFM7	3.113	2.091	2.157	2.137
$Mo_2Ti_2C_3OF$	NM	3.079	2.099	2.138	2.134
	AFM2	3.125	2.113	2.167	2.136

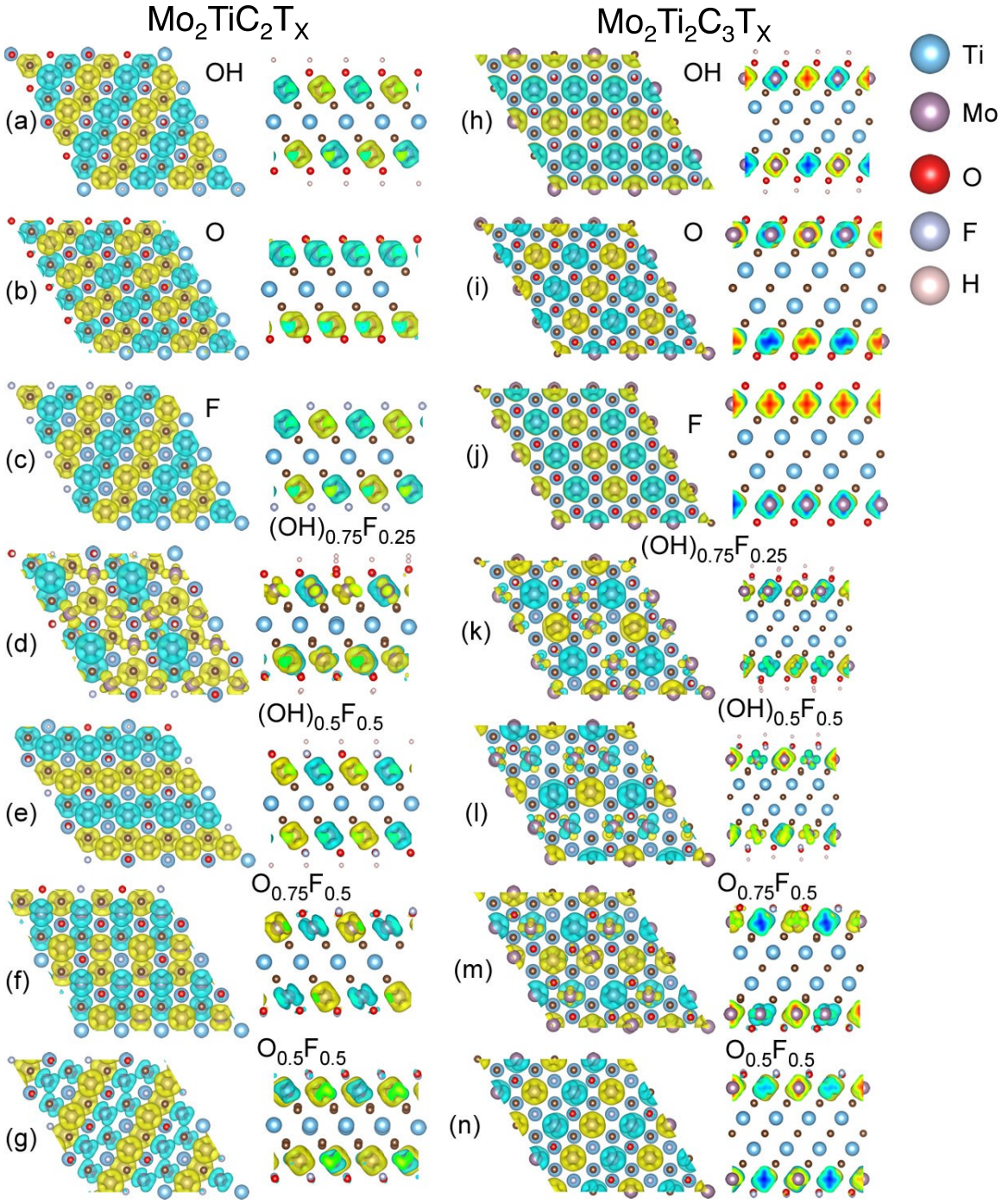

Figure S5. Spatial spin density distributions (up-down) of (a-g) $Mo_2TiC_2T_x$ and (h-n) $Mo_2Ti_2C_2T_x$. Yellow - spin up; blue - spin down.

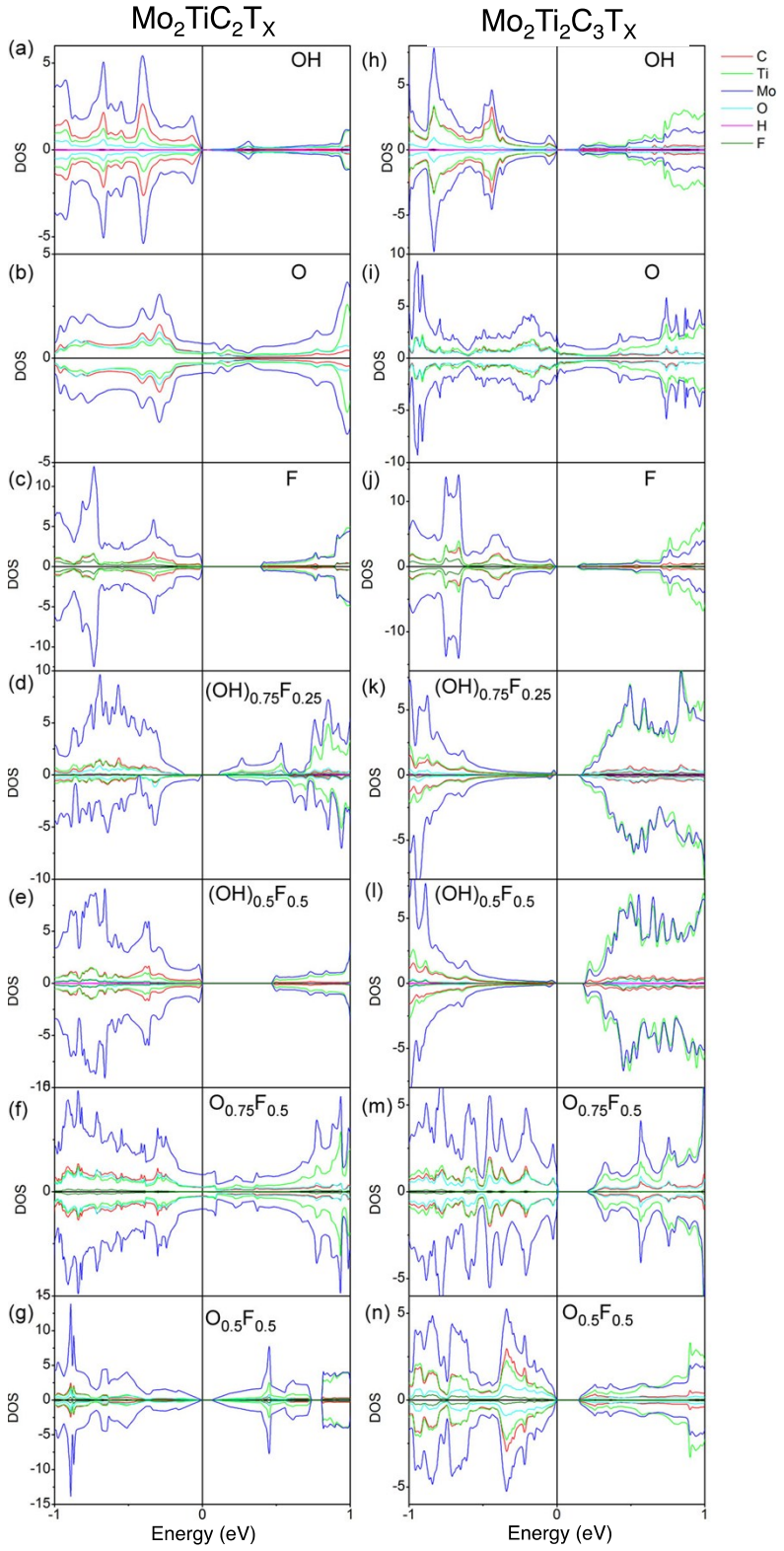

Figure S6. Calculated projected density of states for $Mo_2TiC_2T_x$ (a-g) and $Mo_2Ti_2C_3T_x$ (h-n) MXenes.

References

1. Mott, N. *Journal of Non-Crystalline Solids* 1968, **1**, 1-17.
2. Efros, A.; Shklovskii, B. *Journal of Physics C: Solid State Physics* 1975, **8**, L49.